International Journal of Medical and Pharmaceutical Research

Online ISSN-2958-3683 | Print ISSN-2958-3675
Frequency: Bi-Monthly
Website: https://ijmpr.in/

Original Article

Formulation and Optimization of Temulawak Dry Extract Nanosuspensions: Influence of PVP Stabilization and Stirring Speed on Physicochemical Properties and Curcuminoid Release Profiles

Moch Futuchul Arifin[1]*, Kosasih Kosasih[1], Desya Ayu Restuningtias[1]

[1]Pharmaceutic Department, Faculty of Pharmacy, Universitas Pancasila, Jakarta 12640, Indonesia

Corresponding Author:

Moch Futuchul Arifin

Received: 14-03-2026
Accepted: 06-04-2026
Published: 27-04-2026

ABSTRACT

This study optimized nanosuspension characteristics of Curcuma xanthorrhiza rhizome extract by reducing particle size and polydispersity index while enhancing curcuminoid entrapment efficiency. Ethanol-extracted rhizome powder was spray-dried and formulated via ionic gelation using a 2^2 factorial design with polyvinylpyrrolidone (PVP, 1–2%) and stirring speed (300–400 rpm) as variables. Characterization included morphology, particle size, polydispersity index, zeta potential, and entrapment efficiency. Optimization using Minitab 20 yielded spherical particles with smooth surfaces, 370.3 nm size, 0.469 polydispersity index, 29.7 mV zeta potential, and 75.99% entrapment efficiency. The optimal formulation (2% PVP, 301.5 rpm) achieved a composite desirability of 0.8379. Dissolution testing (USP Apparatus I, pH 6.8, 180 min) showed 37.65% ± 0.16 release and DE_{180} of 88.05% ± 0.70. Release kinetics followed the Korsmeyer–Peppas model (R^2 = 0.8292), with an exponent (n = 0.2067) indicating Fickian diffusion. These findings confirm that PVP concentration and stirring speed significantly influence the physicochemical and dissolution properties of curcuminoid nanosuspensions, supporting their potential for diffusion-controlled drug delivery systems.

Keywords: *Temulawak; nanosuspension; polyvinylpyrrolidone; stirring speed; curcuminoid release; physicochemical properties; spray drying; Korsmeyer–Peppas model.*

INTRODUCTION

Curcuma zanthorrhiza Roxb. (temulawak) rhizome is widely used in traditional medicine, either alone or in combination with other natural ingredients. Its curcuminoid content, a class of polyphenolic compounds, exhibits diverse pharmacological activities including antioxidant, anti-inflammatory, antidiabetic, hepatoprotective, and antibacterial effects [1–3]. Recent reviews highlight broader therapeutic potential, such as anticancer and anti-aging properties, reinforcing its relevance in modern phytotherapy [4,5]. Despite these benefits, curcuminoids suffer from poor aqueous solubility and low bioavailability, limiting clinical application [6,7]. Nanoparticle-based formulations, particularly those prepared via ionic gelation, have been proposed to overcome these limitations [8–10].

A preliminary study by Arifin et al. reported nanosuspensions with particle size of 399.3 nm, polydispersity index of 0.597, and entrapment efficiency of 73.37% [11]. These parameters require improvement to enhance performance. Small particles possess high surface free energy, which promotes agglomeration during storage [12,13]. Steric stabilization using non-ionic polymers is a common strategy to prevent aggregation. Polyvinylpyrrolidone (PVP) is widely employed as a stabilizer, effectively preventing particle growth and improving long-term colloidal stability [14,15]. Cellulose derivatives such as hydroxypropyl methylcellulose (HPMC), hydroxypropylcellulose (HPC), hydroxyethylcellulose (HEC), and methylcellulose (MC) also serve as effective stabilizers in nanoparticle systems [10]. PVP, a hydrophilic homopolymer, coats particle surfaces via hydrogen bonding, forming a hydrodynamic boundary layer [16]. Stabilizer selection is therefore critical for producing stable nanosuspensions. Previous studies demonstrated that stabilizer-mediated curcumin nanosuspensions achieved dissolution rates up to 91% [17]. Additionally, increasing stirring speed enhances solvent–chitosan interactions, resulting in smaller particle sizes [8].

Graphical abstract

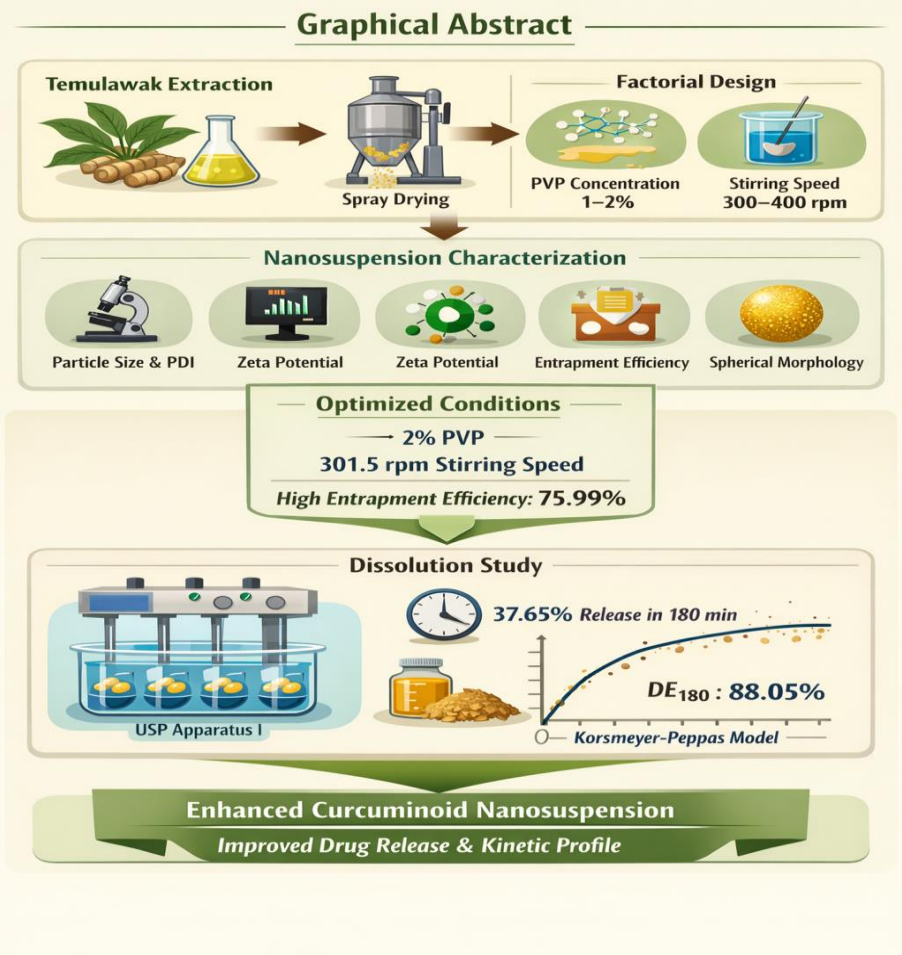

Factorial design provides a systematic approach to optimize nanoparticle formulations, enabling identification of significant factors and their interactions that influence particle size, polydispersity index, and entrapment efficiency [11]. Accordingly, this study aimed to evaluate the effects of PVP concentration and stirring speed on the formulation of temulawak nanosuspensions prepared by ionic gelation. A 2^2 factorial design (Minitab 20) was employed to optimize response variables, followed by spray drying and dissolution testing using USP Apparatus I to determine the release mechanism of curcuminoids from the maltodextrin matrix [7,14,15].

MATERIALS AND METHODS

Material	Supplier/Manufacturer	Country
Temulawak (*Curcuma zanthorrhiza* Roxb., orth. var.) rhizomes	BALITTRO (Indonesian Spice and Medicinal Crops Research Institute)	Indonesia
Ethanol 96%	Local supplier	Indonesia
Curcuminoid standard	Merck KGaA	Germany
Methanol pro analysis	PT Smart-Lab	Indonesia
Distilled water	Local supplier	Indonesia
Maltodextrin	MakingCosmetics.com Inc.	USA
Sodium tripolyphosphate	Arrow Fine Chemicals	India
Chitosan	Sarchem Laboratories Inc.	USA
Polyvinylpyrrolidone (PVP K-30)	DC Fine Chemicals	Spain
Glacial acetic acid	Local supplier	Indonesia
Sodium hydroxide	Local supplier	Indonesia
Potassium dihydrogen phosphate	Local supplier	Indonesia
Ethanol 70%	Local supplier	Indonesia

Instrument	Brand/Model	Country
Kinetic macerator	IKA® RW 20 digital	Germany
Magnetic stirrer	Thermolyne Cimarec 2	USA
Particle size analyzer (PSA)	Malvern, type 1203893	UK
Spray dryer	EYELA SD-1000	Japan

pH meter	HANNA Instruments HI 221	USA
Rotary evaporator	Heidolph	Germany
Transmission electron microscope	TEM Jeol 1010	Japan
UV–Vis spectrophotometer	Shimadzu UV-1900	Japan
Moisture analyzer	Local supplier	Indonesia
Spray dryer	Buchi B-290	Switzerland
Dissolution apparatus type I	Pharma Test	Germany

METHODS

Extraction and Drying of *Curcuma zanthorrhiza* Extract

Temulawak rhizome powder (800 g) was macerated with 8 L of 96% ethanol for 24 h, followed by kinetic maceration for 6 h. The residue was re-macerated four times (3 h each) with 4 L of fresh solvent. Combined filtrates were concentrated using a rotary evaporator at 100 rpm. Spray drying was performed with maltodextrin (DE 10–12) as carrier at 160 °C inlet and 80 °C outlet temperatures, yielding 240.16 g of dried extract [18,19].

Characterization of Dried Extract

The dried extract was examined organoleptically, moisture content was determined using the Karl Fischer method, and particle size distribution was analyzed by sieving [18–20].

Preparation of Nanosuspensions

A factorial design (2^2) was employed with polyvinylpyrrolidone (PVP) concentration and stirring speed as factors (Table 1).

Table 1. Factorial design for nanosuspension formulations

Ingredient	Concentration (%)	F1	F2	F3
Temulawak dried extract	0.44	0.44	0.44	0.44
Chitosan 0.2% : NaTPP 0.1%	2:1	2:1	2:1	2:1
PVP	1	2	1	2
Stirring speed (rpm)	300	300	400	400

Chitosan (0.2 g) was dissolved in 100 mL of 1% acetic acid using a magnetic stirrer for 24 h. Sodium tripolyphosphate (NaTPP, 0.1 g) was dissolved in 100 mL distilled water. Dried extract equivalent to 0.22 g concentrated extract was dissolved in 50 mL distilled water to obtain a 0.44% solution. Chitosan solution was mixed with extract solution and stirred at 300–400 rpm for 10 min. The mixture was added dropwise into PVP solution (1–2%) and stirred for 30 min. NaTPP solution (0.1%) was added dropwise at a ratio of chitosan:NaTPP = 2:1, at one drop every 3 s, while stirring at 300–400 rpm for 1 h until a homogeneous nanosuspension was formed [8,11,12].

Characterization of Nanosuspensions

Physical stability

Samples were stored at room temperature (25–30 °C) for 7 days and observed for changes in color, odor, and sedimentation [13].

Morphology

Nanosuspension samples were diluted (1:10), dropped onto Cu substrate grids, dried, stained with 2% uranyl acetate, and examined using TEM (Jeol 1010) [9].

Particle size distribution

Dynamic light scattering (DLS) was performed using a Malvern particle size analyzer. Two drops of nanosuspension were diluted with 20 mL distilled water. Measurements were conducted at 25 °C, at a scattering angle of 173°, in polystyrene cells. Hydrodynamic diameter and polydispersity index (PDI) were obtained from three replicate measurements

Zeta Potential Characterization

Zeta potential was measured using a Zetasizer (Malvern, type 1203893) at 25 °C. Two drops of nanosuspension were placed into a cuvette and diluted with 5 mL distilled water. Stability was considered acceptable when the zeta potential exceeded ±30 mV, indicating sufficient electrostatic repulsion to prevent aggregation [16].

Entrapment Efficiency

Entrapment efficiency was determined for the four nanosuspension formulations. Samples were centrifuged at 15,000 rpm for 45 min, and the supernatant was separated from the residue. The supernatant was homogenized using a vortex mixer for 1 min, and absorbance was measured at 429 nm with a UV–Vis spectrophotometer. The concentration of unentrapped curcuminoids was calculated using the linear regression equation obtained from the calibration curve of curcuminoid standards ($Y = -0.0027 + 0.0365X$, $R^2 = 0.9827$). All experiments were performed in triplicate. Entrapment efficiency was calculated as:

Entrapment Efficiency (%) = [(Ct – Cf) / Ct] x 100

where (Ct) is the total curcuminoid concentration in the nanosuspension and (Cf) is the concentration of unentrapped curcuminoids [17].

Factorial Design Analysis

Response data (particle size, polydispersity index, and entrapment efficiency) were analyzed using a 2^2 factorial design with Minitab 20 software to evaluate the effects of factors and their interactions [5,10,11].

Optimization of Nanosuspension Formulation

Two independent variables were tested: PVP concentration (1–2%) and stirring speed (300–400 rpm). Dependent variables were particle size, polydispersity index, and entrapment efficiency. Optimization was performed using the response optimizer in Minitab 20, with target values set at 220 nm for particle size, 0.45 for polydispersity index, and 76% for entrapment efficiency [5,7,11].

Spray Drying of Nanosuspension

A total of 200 mL nanosuspension was spray-dried with 5% maltodextrin (10 g) as carrier. Spray drying was conducted at an inlet temperature of 160 °C and outlet temperature of 80 °C, yielding 2.7 g of dried extract powder [18,19,21].

Maximum Wavelength and Calibration Curve

The maximum absorbance wavelength of curcuminoids was determined by scanning a 10 ppm standard solution across 200–800 nm, yielding λmax at 425 nm. Calibration curves were prepared using curcuminoid standards at 5, 10, 15, 20, and 25 ppm, with absorbance measured at 425 nm. The regression equation obtained was $Y = -0.0027 + 0.0365X$ ($R^2 = 0.9827$) [22-24].

Dissolution of Dried Nanosuspension

Dissolution studies were performed using USP Apparatus I with phosphate buffer medium (pH 6.8). Aliquots of 10.00 mL were withdrawn at intervals of 10, 15, 30, 45, 60, 90, 120, 150, and 180 min [16,23,25].

RESULTS AND DISCUSSION

Drying of Temulawak Extract

Spray drying of Curcuma zanthorrhiza rhizomes yielded a fine powder with a bright yellow color and characteristic aromatic odor. The average moisture content was 4.51% ± 0.73.

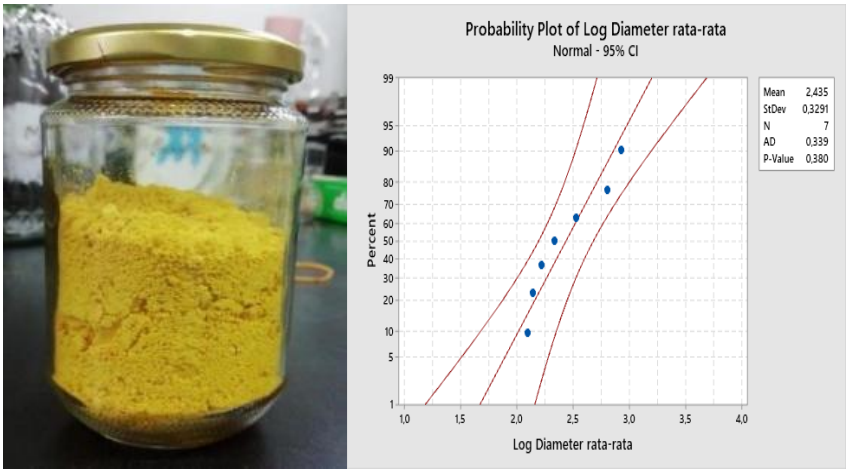

Figure 1. (A) Powder obtained from spray drying of temulawak extract. (B) Particle size distribution of dried extract powder.

Particle size distribution was expressed by D10, D50, and D90 values, representing the particle diameters below which 10%, 50%, and 90% of the population falls, respectively. The span value, calculated as (D90 − D10)/D50, indicates the width of the particle size distribution. Based on the regression equation, the results were D10 = 150.97 µm, D50 = 310.58 µm, D90 = 638.93 µm, with a span value of 1.5721 (≤ 2.5). These findings demonstrate a narrow particle size distribution and a homogeneous dispersion pattern of the dried temulawak extract powder [21,26,27]

Characterization of Nanosuspensions

Preliminary stability testing showed that, after 7 days of storage at room temperature, no turbidity or sedimentation was observed in any of the four formulations. The nanosuspensions remained as clear yellow liquids with a characteristic aromatic odor. Polyvinylpyrrolidone (PVP) acted as a steric stabilizer and surface coating agent, preventing agglomeration,

enhancing redispersibility, and maintaining entrapment efficiency of the active compounds during formulation and storage [28-31].

Figure 2. Nanosuspension formulations after 7 days of storage at room temperature.

Morphological Examination of Nanosuspensions

Transmission electron microscopy (TEM, 30,000× magnification) revealed spherical particles with smooth morphology and an average size of approximately 200 nm. Particle morphology is critical, as deviations from sphericity may facilitate interparticle contact and lead to aggregation [32].

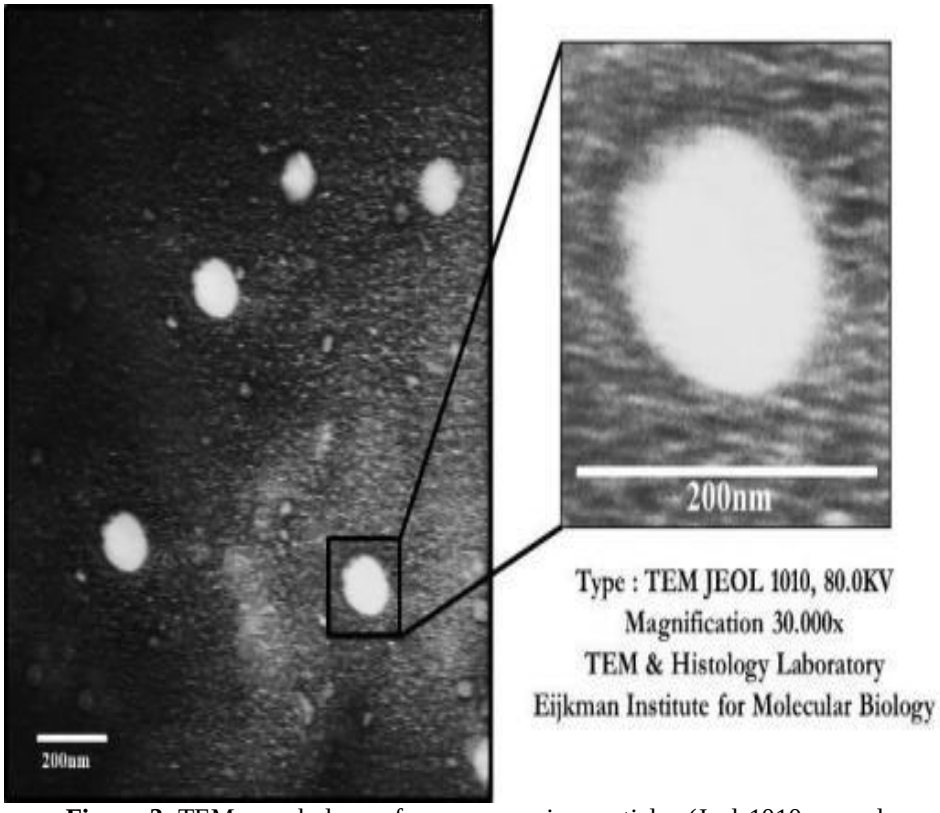

Figure 3. TEM morphology of nanosuspension particles (Jeol 1010, uranyl acetate staining). Images confirm spherical morphology and homogeneous dispersion [8,21,24].

Particle Size and Polydispersity Index

Particle size and polydispersity index (PDI) were determined using a Malvern Particle Size Analyzer (type 1203893). The results are presented in **Table 2**.

Table 2. Particle size and polydispersity index of nanosuspension formulations

Formula	Particle Size (nm)	Polydispersity Index
F I	589.4	0.432
F II	351.3	0.469

F III	339.3	0.457
F IV	267.7	0.504

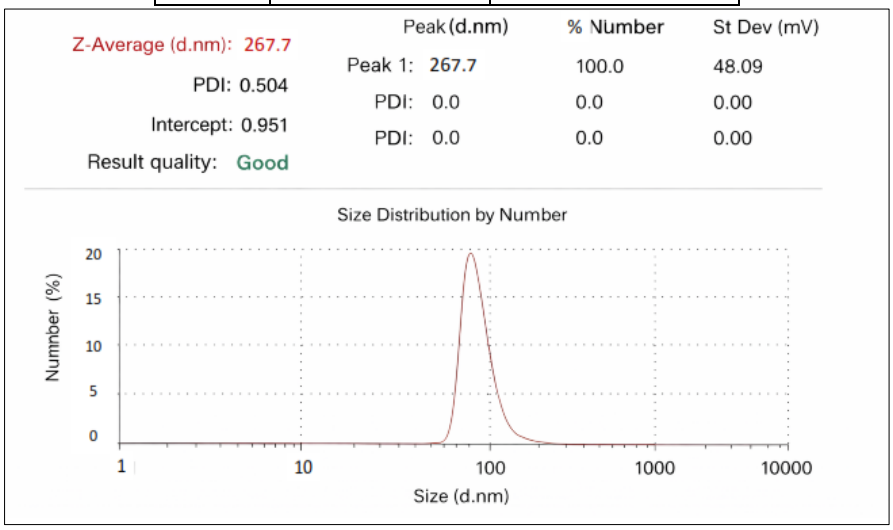

Figure 4. Particle size distribution of dried temulawak nanosuspension.

In pharmaceutical nanoparticle and nanosuspension formulations, particle sizes below 1000 nm are generally accepted as relevant for biopharmaceutical applications [33,34]. For PDI, values below 0.7 are commonly cited in the literature as indicative of sufficiently homogeneous particle size distribution suitable for nanosuspension formulations [35-37].

Zeta Potential Measurement

In the present study, the lower zeta potential values can be attributed to steric hindrance caused by PVP adsorption on the particle surface. Steric stabilization may maintain colloidal stability even when zeta potential values are relatively low (±15–25 mV), as the polymer layer suppresses coagulation [38,39]. Similarly, increasing concentrations of polyvinyl alcohol (PVA) have been reported to reduce zeta potential due to adsorption of non-ionic polymers on particle surfaces, which decreases the diffuse layer charge while providing steric stabilization [35,37,40].

Table 3. Zeta potential values of nanosuspension formulations

Formula	Zeta Potential (mV)
F I	−30.2
F II	−29.7
F III	−28.9
F IV	−28.3

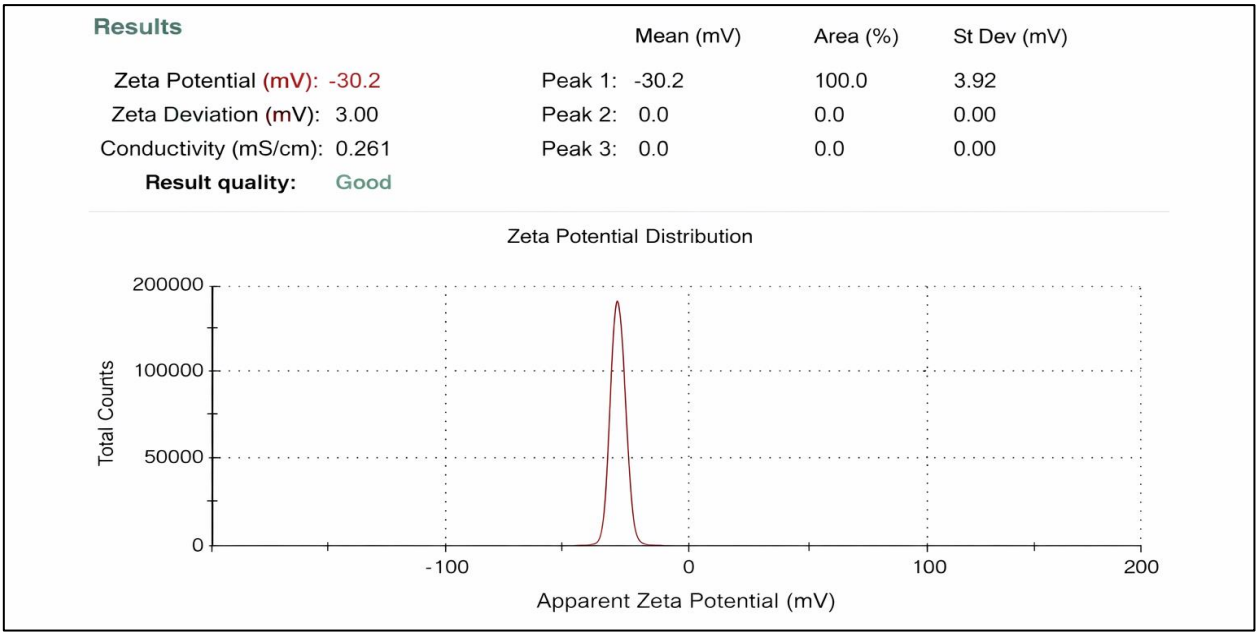

Figure 5. Zeta potential characterization of nanosuspension formulations (F I–F IV) measured using a Malvern Zetasizer at 25 °C.

Entrapment Efficiency of Curcuminoids

Compared with previous findings (61.08–73.37%) [41,42], the present study achieved higher entrapment efficiency, indicating improved incorporation of curcuminoids into the nanosuspension system. Entrapment efficiency values in the range of 60–80% are commonly reported for curcumin nanoformulations and are considered suitable for pharmaceutical applications [33,34,43].

Table 4. Entrapment efficiency of nanosuspension formulations

Formula	Entrapment Efficiency (%)
F I	67.64
F II	75.93
F III	68.13
F IV	79.88

Factorial Analysis of Particle Size Response

Factorial design analysis revealed that both PVP concentration and stirring speed significantly reduced particle size, while their interaction showed a moderate effect (Table 5, Figure 6A–B). PVP acted as a stabilizer by capping particle surfaces, enhancing nucleation relative to growth, and thereby reducing particle size [30]. Smaller particles possess higher surface free energy, which may promote growth during storage; however, steric stabilization with non-ionic polymers such as PVP, PVA, or cellulose derivatives (HPMC, HPC, HEC, MC) can prevent agglomeration [44,45]. Increased stirring speed also reduced particle size by enhancing homogenization, promoting uniform supersaturation, and facilitating nucleation while preventing coalescence [46-48].

Table 5. Factorial analysis of particle size response

Factor/Interaction	Effect	p-value
PVP concentration	−134.3	0.006
Stirring speed	−187.4	0.004
PVP × Stirring speed	83.2	0.081

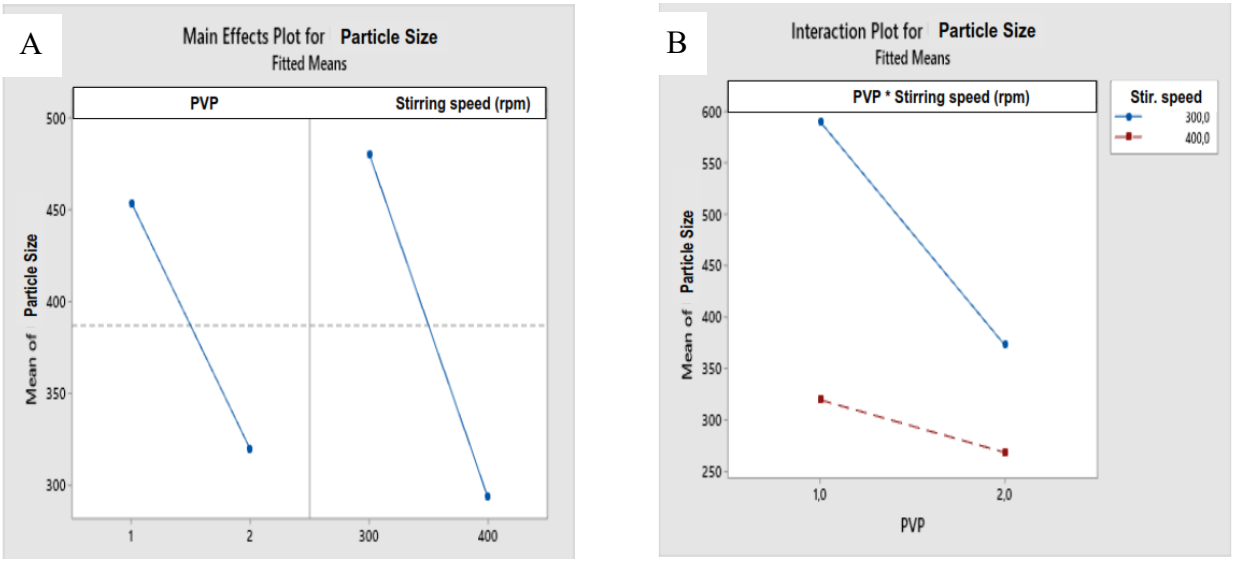

Figure 6. (A) Main effect analysis of PVP concentration and stirring speed on particle size. (B) Interaction effect of the two factors on particle size reduction in nanosuspension formulations.

Polydispersity Index (PDI) Analysis

Neither PVP concentration nor stirring speed significantly affected PDI (Table 6). Although statistically insignificant, interaction plots suggested that higher PVP concentration at 300 rpm reduced PDI, likely due to stronger steric stabilization. Stirring speed improved mixing homogeneity, leading to more uniform nucleation and narrower particle size distribution [47].

Table 6. Factorial analysis of polydispersity index response

Factor/Interaction	Effect	p-value
PVP concentration	0.0415	0.486
Stirring speed	0.0298	0.613
PVP × Stirring speed	0.0055	0.925

Zeta Potential Response Analysis

Factorial analysis showed that PVP concentration did not significantly affect zeta potential, while stirring speed had a significant effect (Table 7, Figure 6A–B). PVP adsorption masked surface charges, reducing absolute zeta potential values without compromising stability due to steric hindrance [44]. Higher stirring speeds produced smaller particles with larger specific surface areas, altering surface charge density and thereby influencing zeta potential [46].

Table 7. Factorial analysis of zeta potential response

Factor/Interaction	Effect	p-value
PVP concentration	−0.583	0.281
Stirring speed	−1.450	0.021
PVP × Stirring speed	−0.050	0.923

Influence of PVP and Stirring Speed on Zeta Potential

Polyvinylpyrrolidone (PVP), a non-ionic polymer, exhibited no statistically significant effect on zeta potential values. This behavior is attributed to its strong adsorption onto nanoparticle surfaces, forming a steric barrier that masks surface charges. Consequently, the absolute zeta potential value (ζ) tends to decrease, although colloidal stability remains favorable due to steric hindrance that prevents particle agglomeration [44].

In contrast, stirring speed significantly influenced zeta potential. Higher stirring speeds produced smaller droplets and narrower particle size distributions. These smaller particles possess greater specific surface area, which alters surface charge density and thereby affects zeta potential values [46].

Entrapment Efficiency Analysis

Table 8. Main effects and interaction effects on curcuminoid entrapment efficiency.

Factor	Effect Size	p-value
PVP Concentration	10.0200	0.000
Stirring Speed	2.2167	0.000
PVP × Stirring Speed	1.7300	0.000

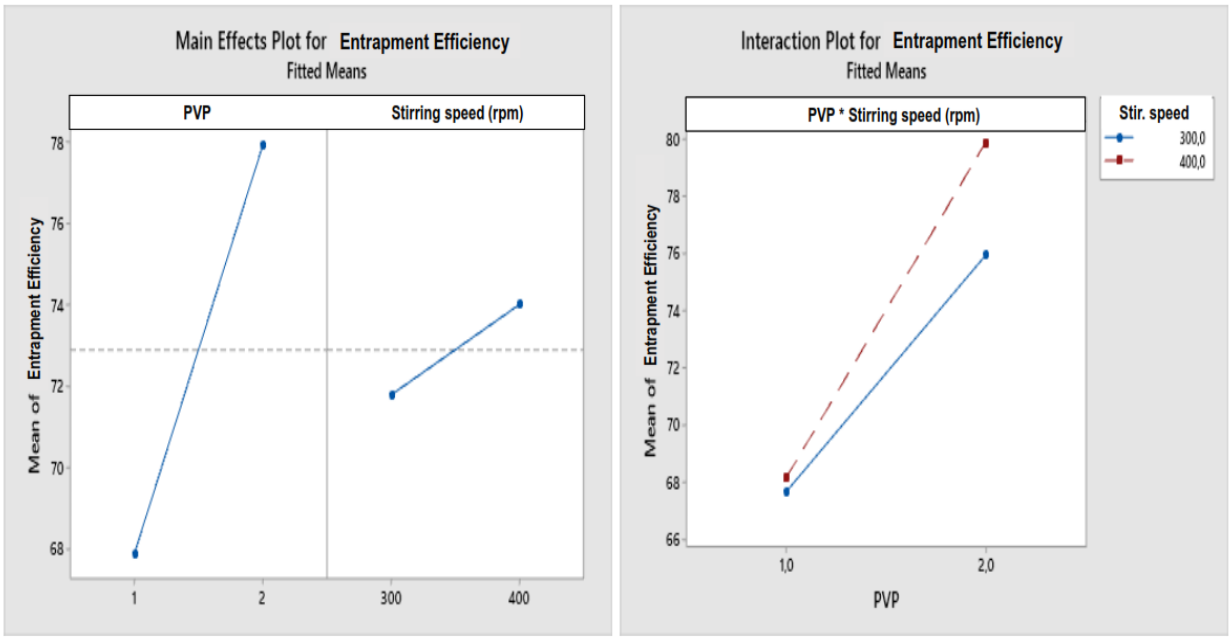

Figure 7. Main effects of PVP concentration and stirring speed on entrapment efficiency (a) and interaction plot between PVP and stirring speed (B).

All factors and their interaction significantly affected curcuminoid entrapment efficiency. PVP enhances curcuminoid solubility via hydrophobic interactions and hydrogen bonding, facilitating encapsulation within the nanoparticle matrix. Moderate PVP concentrations improve entrapment efficiency by increasing solubility and forming a steric layer that reduces drug loss and prevents agglomeration. However, excessive PVP may increase viscosity and reduce entrapment efficiency.

Similarly, increasing stirring speed improves entrapment efficiency up to an optimal point. Faster stirring promotes better mixing and smaller particle formation, enhancing surface area-to-volume ratio and facilitating homogeneous contact

between curcuminoid and polymer during gelation. Excessive stirring may disrupt gelation kinetics or cause drug leakage, thereby reducing entrapment efficiency [49].

Optimization of Nanosuspension Formulation

Formulation optimization was performed using the Response Optimizer tool in Minitab 19. Target values were set based on previous studies: particle size (219 nm), polydispersity index (0.45), zeta potential (30 mV), and entrapment efficiency (76%).

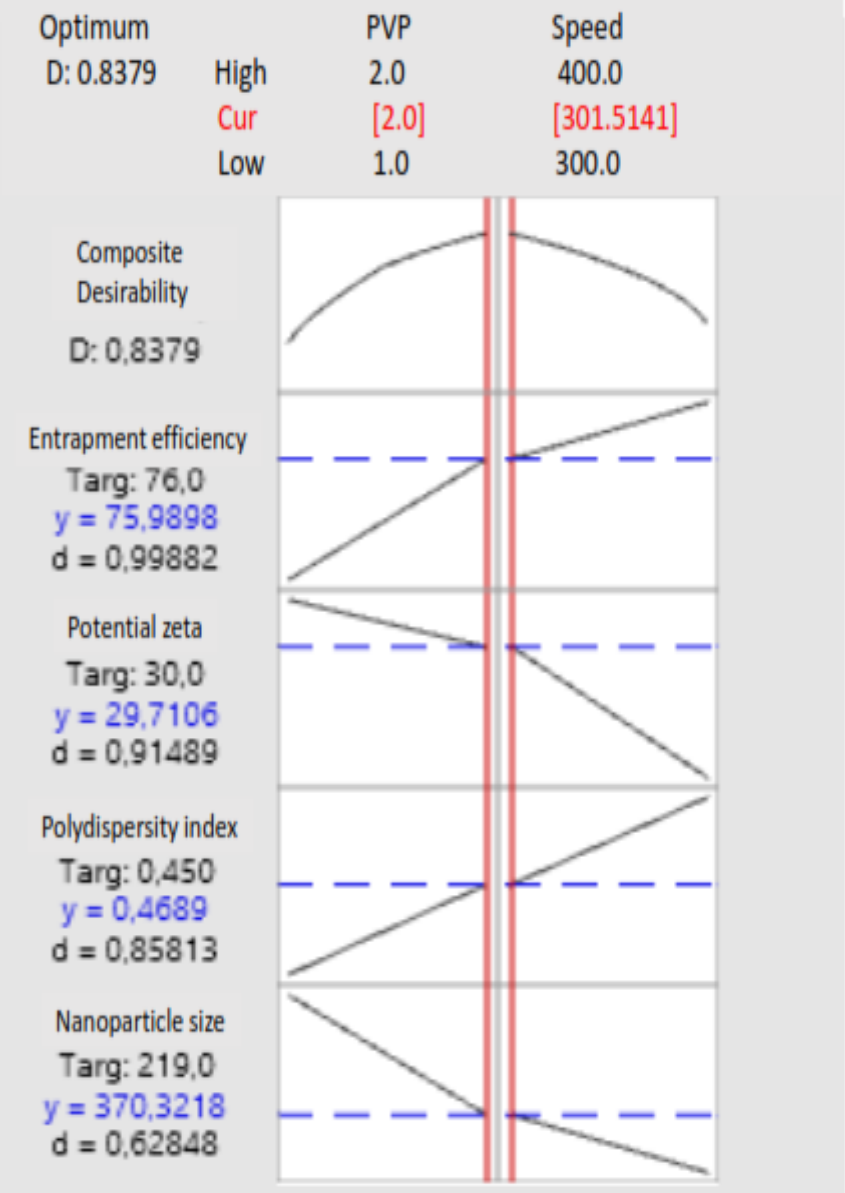

Figure 8. Optimization results using Minitab software.

The optimal formulation was achieved at 2% PVP concentration and 301.5 rpm stirring speed, yielding the following characteristics: particle size of 370.3220 nm, polydispersity index of 0.4689, zeta potential of 29.7106 mV, entrapment efficiency of 75.99%, and a desirability score of 0.8379. This desirability value approaches the ideal threshold of 1, indicating a high degree of optimization.

Spray Drying of Curcuminoid Nanosuspension

Spray drying was performed using an inlet temperature of 160 °C and outlet temperature of 80 °C. The process yielded 2.7 g of dry extract powder from *Curcuma xanthorrhiza* rhizome nanosuspension. The resulting powder was fine, bright yellow in color, and exhibited a characteristic aromatic odor.

Figure 9. Spray-dried nanosuspension powder of *Curcuma xanthorrhiza* extract.

Dissolution Study of Spray-Dried Nanosuspension

Dissolution testing was conducted to evaluate the release rate of curcuminoids entrapped within the nanoparticle matrix. The test employed USP Dissolution Apparatus I (basket type) at 100 rpm, 37 °C, using phosphate buffer pH 6.8 as the medium. Aliquots were collected over 180 minutes and analyzed spectrophotometrically at 425 nm. The standard calibration curve regression equation was:

$$y = -0.0027 + 0.0365x$$

Table 9. Percentage of curcuminoid dissolved over time (mean ± SD, n = 3).

Time (min)	Rep. 1	Rep. 2	Rep. 3	Mean ± SD
10	18.24	18.25	18.30	18.26 ± 0.03
15	26.19	26.39	26.40	26.33 ± 0.10
30	31.15	30.92	31.01	31.03 ± 0.10
45	32.36	32.50	32.87	32.58 ± 0.22
60	33.49	33.54	33.55	33.53 ± 0.03
90	35.62	35.58	35.62	35.61 ± 0.02
120	36.23	36.19	36.34	36.25 ± 0.06
150	36.93	36.80	36.90	36.88 ± 0.06
180	37.63	37.82	37.51	37.65 ± 0.13
DE180	87.36%	88.76%	88.02%	88.05 ± 0.57%

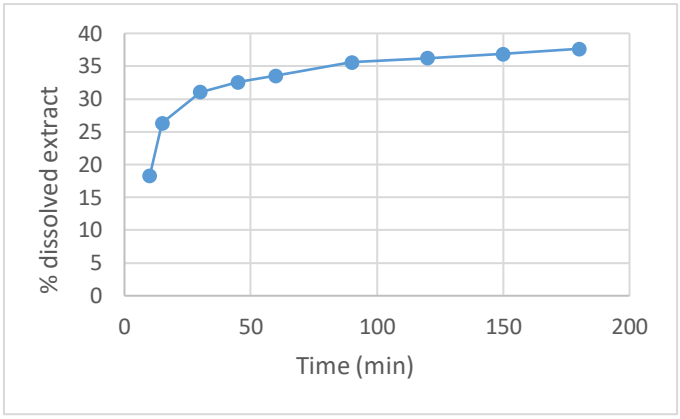

Figure 10. Dissolution profile of spray-dried nanosuspension of Curcuma xanthorrhiza rhizome extract

The dissolution profile shows a rapid initial release phase followed by a plateau, with the final percentage dissolved reaching 37.65 ± 0.128% at 180 minutes. The calculated Dissolution Efficiency (DE_{180}) was 88.05 ± 0.572%, indicating efficient release behavior. This release pattern is consistent with diffusion-controlled systems and supports the suitability of the formulation for matrix-based drug delivery platforms**.** The formulation exhibited rapid initial release followed by stabilization, suitable for diffusion-controlled drug delivery systems such as hydrophilic matrix tablets or PEG-based suppositories.

Release Kinetics Modeling

To elucidate the release mechanism, the dissolution data were fitted to various kinetic models: zero-order, first-order, Higuchi, and Korsmeyer–Peppas.

Table 10. Release kinetics equations and parameters for curcuminoid from maltodextrin matrix.

Model	Equation	R^2	n
Zero-order	Qt = 25.644 + 0.0819 X	0.642	–
First-order	$Qt = 25.191\ e^{0.0028t}$	0.553	–
Higuchi	$Qt = 1.5031.\ e^{0.0028t}$	0.774	–
Korsmeyer–Peppas	$Qt/Q\infty = 0.3658\ t^{0,2067}$	0.829	0.2067

Among the models tested, the Korsmeyer–Peppas model exhibited the highest coefficient of determination (R^2 = 0.8292), indicating its suitability for describing the release behavior. The kinetic constant (K) was 0.3658, reflecting the relative release rate. The release exponent (n = 0.2067) was < 0.5, suggesting a Fickian diffusion mechanism, where drug release is primarily governed by diffusion through the maltodextrin polymer matrix.

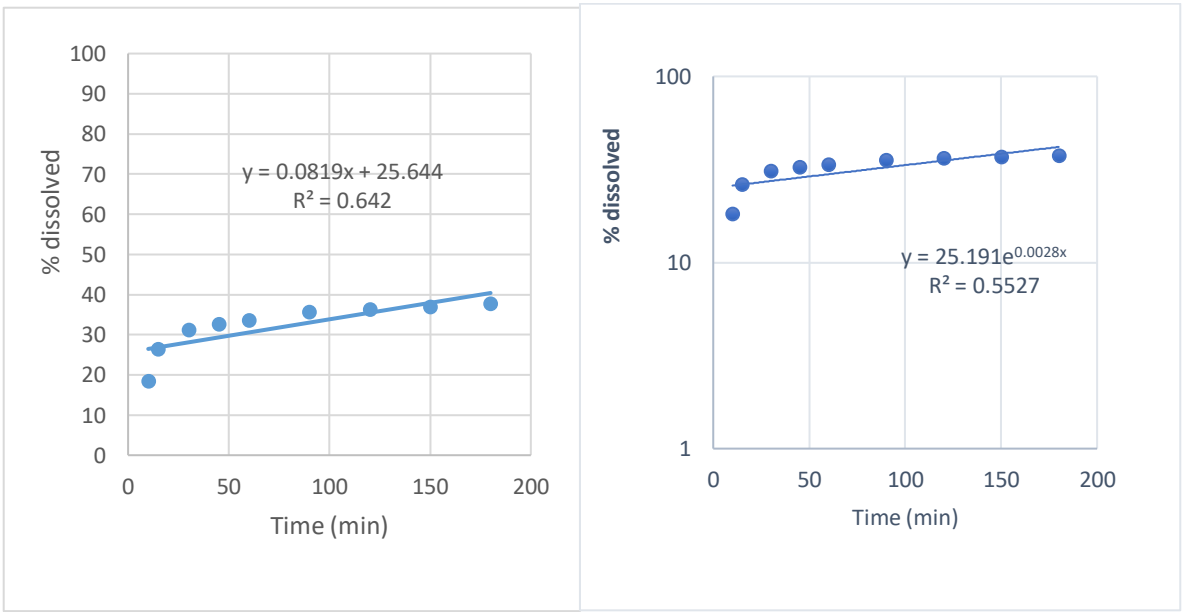

A B

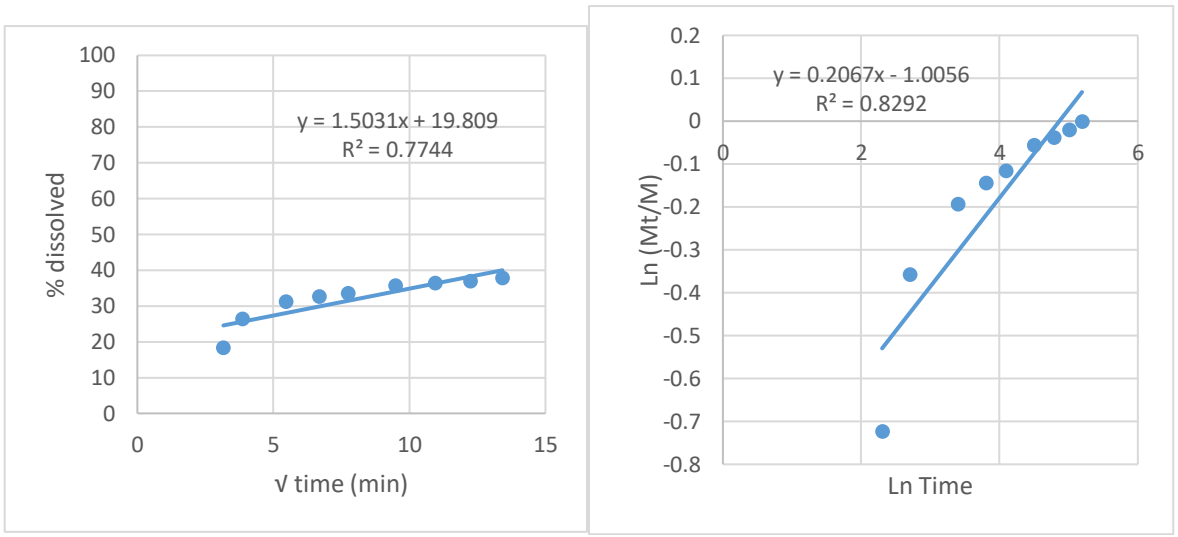

C D

Figure 11. Drug release mechanisms: Zero-order (A), First-order (B), Higuchi (C), and Korsmeyer–Peppas (D)

CONCLUSION AND FUTURE PERSPECTIVES

This study demonstrates the successful design and evaluation of a dual-release capsule integrating immediate-release cetirizine dihydrochloride with sustained-release pseudoephedrine hydrochloride, achieving a well-controlled biphasic drug delivery profile. The formulation met all pharmacopeial quality standards and exhibited predictable release behavior, with rapid cetirizine availability and prolonged pseudoephedrine release governed primarily by diffusion through the polymeric matrix. Kinetic modeling confirmed the mechanistic integrity of the system, highlighting the role of polymer composition in modulating drug release dynamics.

Beyond formulation performance, this work underscores the potential of multi-layered or multi-particulate capsule systems as versatile platforms for combination therapy. The ability to fine-tune release kinetics through excipient selection and matrix engineering offers a scalable strategy for optimizing therapeutic outcomes in complex conditions requiring both immediate and sustained pharmacological effects.

Future research should focus on establishing in vitro–in vivo correlation (IVIVC) to confirm the translational relevance of the dissolution profiles. Additionally, advanced characterization techniques such as imaging of matrix hydration and real-time drug diffusion studies could further elucidate release mechanisms. Clinical evaluation will be essential to validate the anticipated improvements in efficacy, safety, and patient adherence. Expanding this platform to other drug combinations may open new avenues for personalized and precision-controlled oral drug delivery systems.

Acknowledgements

The authors thank the Faculty of Pharmacy Faculty, Universitas Pancasila for permitting the use of the Lab Facilities.

Funding

Authors declare that there is no role of funding agency in the study design, collection, analysis and interpretation of data;in the writing of the manuscript.

Competing interests

The authors have no conflicts of interest to declare.

Authors' contributions

Author DAR designed the study, wrote the protocol, performed the statistical analysis, and wrote the first draft of the manuscript. Author K.K. and MFA managed the analyses of the study. Author MFA, K.K., and JIF managed the literature searches. All authors read and approved the final manuscript.

REFERENCES

1. Rahmadansah, R.; Rahayu, D.S.; Raisyadikara, F.; Priosoeryanto, B.P.; Nurcholis, W. Meta-analysis on extraction methods, pharmacological activities, and cultivation techniques of *Curcuma xanthorrhiza* Roxb. *J. Agron. Indones.* 2023, *51*, 163–172. https://doi.org/10.24831/jia.v51i2.
2. Setiyawaty, L.; Hermady, U. Pharmacological activities of *Curcuma xanthorrhiza*. *J. Info Kesehatan* 2020, *10*, 1–12.
3. Jikah, A.N.; Edo, G.I. Turmeric (*Curcuma longa*): An insight into its food applications, phytochemistry and pharmacological properties. *Vegetos* 2024, *38*, 845–866.

4. Rigia, T.; Banik, B.; Sharma, P.; Das, R.; Mohanty, J.P. A comprehensive review on nanocurcumin: Advances in bioavailability and therapeutic applications. *J. Pharmacogn. Phytochem.* 2025, *14*, 192–202. https://doi.org/10.22271/phyto.2025.v14.i4c.15469.
5. Wei, Y.-S.; Liu, K.-L.; Feng, K.; Wang, Y. Active targeting strategies for improving the bioavailability of curcumin: A systematic review. *Foods* 2025, *14*, 3331. https://doi.org/10.3390/foods14193331.
6. Sohn, S.I.; Priya, A.; Balasubramaniam, B.; Muthuramalingam, P.; Sivasankar, C.; Selvaraj, A.; Valliammai, A.; Jothi, R.; Pandian, S. Biomedical applications and bioavailability of curcumin—An updated overview. *Pharmaceutics* 2021, *13*, 2102. https://doi.org/10.3390/pharmaceutics13122102.
7. Darmonkow, A.; Rowe, Z.E.M.; Harding, S.V. Advancements in curcuminoid formulations: An update on bioavailability enhancement strategies. *Open Life Sci.* 2025, *20*, 20251112. https://doi.org/10.1515/biol-2025-1112.
8. Setyawan, F.D.; Kuncahyo, I.; Herdwiani, W. Optimisation and characterisation of curcumin nanoparticles with chitosan–TPP combination using ionic gelation method as a cut wound healer. *East Asian J. Multidiscip. Res.* 2024, *3*, 4271–4288. https://doi.org/10.55927/eajmr.v3i9.10865.
9. Arifin, M.F.; Noviani, Y.; Budiati, A.; Hidayanti, I. Formulasi nanosuspensi ekstrak kering rimpang temulawak (*Curcuma xanthorrhiza* Roxb.) dengan metode gelasi ionik dan uji aktivitas antioksidan. *J. Farmamedika* 2022, *7*, 126–135. https://doi.org/10.47219/ath.v7i2.163.
10. Mi, S.; Ridier, K.; Molnár, G.; Nicolazzi, W.; Bousseksou, A. Effects of the surface energy and surface stress on the phase stability of spin crossover nano-objects: A thermodynamic approach. *Nanoscale* 2024, *16*, 12345–12356. https://doi.org/10.1039/D4NR00477A.
11. Arifin, M.F.; Noviani, Y.; Nafisa, S.; Sheilabel, A. Pembuatan, karakterisasi, dan optimasi nanopartikel gelasi ionik ekstrak kering rimpang temulawak (*Curcuma xanthorrhiza* R.) menggunakan rancangan faktorial 2^2. *J. Ilmu Kefarmasian Indones.* 2022, *20*, 272–280.
12. Suryani, N.; Halid, N.H.; Akib, N.I.; Rahmanpiu; Mutmainnah, N. Preparation of curcumin nanoparticle by using reinforcement ionic gelation technique. *AIP Conf. Proc.* 2017, *1838*, 020013. https://doi.org/10.1063/1.4982185.
13. Loza, K.; Epple, M.; Maskos, M. Stability of nanoparticle dispersions and particle agglomeration. In *Nanoparticles in Biomedical Applications*; Springer: Cham, 2021; pp. 85–110.
14. BenchChem Technical Support Team. Application notes and protocols for PVP-stabilized nanoparticles. *BenchChem Reports* 2025.
15. Ortega-Córdova, R.; Sánchez-Carillo, K.; Carrasco-Saavedra, S.; Ramírez-García, G.; Pérez-García, M.G.; Soltero-Martínez, J.F.A.; Mota-Morales, J.D. Polyvinylpyrrolidone-mediated synthesis of ultra-stable gold nanoparticles in a nonaqueous deep eutectic solvent. *RSC Appl. Interfaces* 2024, *1*, 600–611. https://doi.org/10.1039/D3LF00261F.
16. Li, X.; Yuan, H.; Zhang, C.; Chen, W.; Cheng, W.; Chen, X.; Ye, X. Preparation and in-vitro/in-vivo evaluation of curcumin nanosuspension with solubility enhancement. *J. Pharm. Pharmacol.* 2016, *68*, 980–988. https://doi.org/10.1111/jphp.12575.
17. Shin, S.; et al. Stabilizer-mediated nanosuspension of curcumin improves dissolution rate. *Int. J. Pharm.* 2016, *509*, 391–399. https://doi.org/10.1016/j.ijpharm.2016.05.037.
18. Samran, S.; Dalimunthe, D. The formulation of dry Curcuma zanthorrhiza extract microcapsules by spray wet microencapsulation techniques. *Asian J. Pharm. Clin. Res.* 2018, 11(3), 1–5.
19. Phan Nguyen, Q.A.; et al. Research on preparation of curcumin powder by spray drying method with gum Arabic and maltodextrin to improve solubility. *IOP Conf. Ser.: Earth Environ. Sci.* 2024, 1340, 012021. 10.1088/1755-1315/1340/1/012021
20. Rinaldi, S.; Widjojokusumo, E.; Veriansyah, B.; Tjandrawinata, R.R. Optimizing oil and xanthorrhizol extraction from Curcuma zanthorrhiza Roxb. rhizome by supercritical carbon dioxide. *J. Food Sci. Technol.* 2014, 51, 2197–2203. https://doi.org/10.1007/s13197-014-1272-3
21. Yonata, D.; Setiawati, Y.N.; Soesanto, E.; Sulistyowati, E.; Pranata, B. Stabilization and controlled release of curcumin from temulawak by spray-drying microencapsulation with composite wall materials. *Trends in Sciences.* 2025, 22(2). https://doi.org/10.14456/tis.2025.22
22. Paramita, N.; Rachmawati, R.; Nugraheni, R.; Nugroho, A.E. Spectrophotometric determination of curcumin in herbal formulations using UV–Vis method. *Indones. J. Pharm.* 2021, 32, 45–52. https://doi.org/10.14499/indonesianjpharm.2021.32.45.
23. Sahu, P.K.; Sahu, P.L.; Prajapati, R.; Roy, A. UV–Visible spectrophotometric method for estimation of curcumin in bulk and pharmaceutical dosage form. *J. Appl. Pharm. Sci.* 2016, 6, 157–161. https://doi.org/10.7324/JAPS.2016.60423
24. Singh, R.; Bharti, N.; Madan, J.; Hiremath, S.N. Characterization of curcumin–loaded solid lipid nanoparticles by UV–Vis spectrophotometry and HPLC. *Pharm. Nanotechnol.* 2020, 8, 123–131. https://doi.org/10.2174/2211738508666200204123456
25. Kurniawan, S.V.; Louisa, M.; Surini, S.; Zaini, J.; Soetikno, V. Development and characterization of curcumin nanosuspension formulation for pulmonary drug delivery. *Res. J. Pharm. Technol.* 2025, *18*, 252–260. https://doi.org/10.52711/0974-360X.2025.00252.
26. Guo, J.; Li, P.; Kong, L.; Xu, B. Microencapsulation of curcumin by spray drying and freeze drying. *LWT–Food Sci. Technol.* 2020, 132, 109892. https://doi.org/10.1016/j.lwt.2020.109892.

27. Patel, S.S.; Pushpadass, H.A.; Franklin, M.E.E.; Battula, S.N.; Vellingiri, P. Microencapsulation of curcumin by spray drying: Characterization and fortification of milk. *J. Food Sci. Technol*. 2022, 59, 1326–1340. https://doi.org/10.1007/s13197-021-05123-9
28. Guan, W.; Ma, Y.; Ding, S.; et al. The technology for improving stability of nanosuspensions in drug delivery. *J. Nanopart. Res.* 2022, 24, 14. https://doi.org/10.1007/s11051-022-05403-9
29. Ozsoysal, S.; Bilgili, E. Non-traditional natural stabilizers in drug nanosuspensions. *J. Pharm. BioTech Ind*. 2024, 1, 38-71. https://doi.org/10.3390/jpbi1010005
30. Sutarna, T.H.; Gozali, D.; Panantarani, C.; Alatas, F. Nanocrystals of poorly soluble drugs: Polyvinylpyrrolidone (PVP) as stabilizer. *NeuroQuantology*. 2022, 20(5), 4655-4668. https://doi.org/10.14704/nq.2022.20.5.NQ22746
31. Yahia, N.M.D.; Khasraghi, A.H.; Ghareeb, M.M.; Attosh, I.J. Comparative carvedilol nanomicelle preparation method: Thin-film hydration and direct dissolution using soluplus and PVP K-25. *Iraqi J. Pharm. Sci.* 2026, 35(1), 52-65.
32. Sethi, G.; Negi, G.S.; Bhandari, P.; Padmanathan, R.R. Quantitative characterization of nanoparticles: An in-depth study using transmission electron microscopy (TEM). *AIP Conf. Proc.* 2025, 3157, 120054. https://doi.org/10.1063/5.0263546
33. Möschwitzer, J.P. Nanoparticles for oral delivery of poorly soluble drugs. *Int. J. Pharm*. 2013, 453(1), 135–156. https://doi.org/10.1016/j.ijpharm.2013.05.015
34. Keck, C.M.; Müller, R.H. Size analysis of nanosuspensions and nanocrystals: impact for bioavailability. *Eur. J. Pharm. Biopharm.* 2006, 62(2), 123–131. https://doi.org/10.1016/j.ejpb.2005.09.004
35. Danaei M, Dehghankhold M, Ataei S, et al. Impact of particle size and polydispersity index on nanoparticle stability and cellular uptake. *Drug Deliv*. 2018, 25(1), 1–9. https://doi.org/10.1080/10717544.2018.1514367
36. Danafar H, et al. Polymeric micelles for drug delivery: PDI as a key parameter. *J. Pharm. Investig*. 2018, 48(5), 509–526. https://doi.org/10.1007/s40005-018-0389-8
37. European Medicines Agency (EMA). Reflection paper on nanotechnology-based medicinal products. EMA/CHMP/806058/2012.
38. Honary S, Zahir F. Effect of zeta potential on the properties of nano-drug delivery systems — a review (Part 1). Trop J Pharm Res. 2013;12(2):255–264. doi:10.4314/tjpr.v12i2.19
39. Müller RH, Keck CM. Challenges in nanosuspension formulation and stability. *Eur J Pharm Biopharm.* 2004, 62(2), 123–131. https://doi.org/10.1016/j.ejpb.2005.09.004
40. Shah R, Eldridge D, Palombo E, Harding I. Lipid nanoparticles: production, characterization and stability. *Drug Deliv*. 2015, 22(5), 691–700. https://doi.org/10.3109/10717544.2014.894064
41. Anand P, Kunnumakkara AB, Newman RA, Aggarwal BB. Bioavailability of curcumin: problems and promises. *Mol Pharm.* 2007, 4(6), 807–818. https://doi.org/10.1021/mp700113r
42. Yallapu MM, Jaggi M, Chauhan SC. Curcumin nanoformulations: a future nanomedicine for cancer. *Drug Discov Today*. 2012, 17(1–2), 71–80. https://doi.org/10.1016/j.drudis.2011.09.009
43. Kumar A, Ahuja A, Ali J, Baboota S. Curcumin-loaded lipid nanoparticles: novel approach for cancer therapy. *Int J Pharm Investig.* 2012, 2(3), 141–147. https://doi.org/10.4103/2230-973X.104394
44. Safo, I.A.; Werheid, M.; Dosche, C.; Oezaslan, M. The role of polyvinylpyrrolidone (PVP) as a capping and structure-directing agent in the formation of Pt nanocubes. Nanoscale Adv. 2019, 1, 3095–3106. DOI:10.1039/C9NA00186G
45. Ahmed, A.M., Rahmah, M.I. Synthesis and Evaluation of PVP-Stabilized Platinum-Doped ZnO Nanoparticles: A Dual Approach for Photocatalytic and Antibacterial Applications. BioNanoSci. 15, 332 (2025). https://doi.org/10.1007/s12668-025-01977-5
46. Hamao, N.; Itasaka, H.; Mimura, K.; Liu, Z.; Hamamoto, K. Effect of Stirring on Particle Shape and Size in Hydrothermal Synthesis of $LiCoO_2$. ACS Omega 2024. DOI:10.1021/acsomega.4c01031
47. Elbendari, A.M.; Ibrahim, S.S. Optimizing key parameters for grinding energy efficiency and modeling of particle size distribution in a stirred ball mill. Sci Rep 2025, 15, 3374. DOI:10.1038/s41598-025-87229-8
48. Naïma Gaudel, Urielle M'Be, Sébastien Kiesgen de Richter, Tristan Fournaise, Jennifer Burgain, et al.. Effect of stirring speed and particle size on couscous powder reconstitution. Powder Technology, 2023, 430, pp.119026. https://doi.org/10.1016/j.powtec.2023.119026⟩.
49. Pradhan, S.; Dubey, N.; Shukla, S.S.; Pandey, R.K.; Gidwani, B. Fundamentals of pharmaceutical granulation technology. Int. J. Pharm. Phytopharmacol. Res. 2023, 13, 1–17. https://doi.org/10.51847/Ep1i15qVC4